

Transverse Vibration analysis of Hydro-generator Assembly

Madhav Baral ^a, Kamal Pokharel ^b, Mahesh Chandra Luintel ^c

^{a, b} Department of Automobile and Mechanical Engineering, Thapathali Campus, IOE, Tribhuvan University, Nepal

^c Department of Mechanical and Aerospace Engineering, Pulchowk Campus, IOE, Tribhuvan University, Nepal

✉ ^a madav.078msedm08@tcioe.edu.np, ^b k.pokharel@tcioe.edu.np, ^c mcluintel@ioe.edu.np

Abstract

In this study, the natural frequency for different mode of the transverse vibration for the hydro generator assembly supported on the elastic bearing are analysed with the help of mathematical approach namely transfer matrix method. For the formulation of transfer matrix of the shaft, two different beam theory i.e Euler-Bernoulli Beam theory and Timoshenko Beam theory are considered. The solutions obtained with these considerations are compared with the results obtained from the Finite Element method(FEM) to evaluate the reliability of the mathematical approach. As per the calculations, the natural frequency with Euler Bernoulli beam model for first three modes are 17.46 Hz, 57.83 Hz and 87.65 Hz and the same for Timoshenko beam model are 17.32 Hz, 56.12 Hz and 82.07 Hz. From FEM, the natural frequency calculated for first three modes are 20.01 Hz, 49.9 Hz and 90.54 Hz. The results obtained with both the beam theory are close to the result obtained from Finite element method however, the results obtained from the Timoshenko beam concept are more close to the results from FEM for two flexural vibration mode due to the consideration of the shear deformation and inertial property of the beam.

Keywords

Natural Frequency, Transverse vibration, Transfer Matrix, Euler-Bernoulli Beam, Timoshenko Beam, Shear Deformation

1. Introduction

Most of the power generating units comprises of disk connected to the shaft. One prevalent instance of such machinery is the hydro turbine generator assembly, utilized for generating electricity in hydroelectric power plants. Vibration of hydro turbine generating system strongly influences the safety of the powerhouse where turbines are installed. Thus, the safe and stable operation of hydro power station is becoming increasingly significant in engineering practice. It has profound significance to explore the vibration causes and vibration characteristics of the generating unit to take more precise protective measures to ensure the optimal operation of the hydro power station.

For a hydro generator assembly unit, the vibration aroused due to bending generally has more relevance than vibration due to torsion [1]. To evaluate the natural frequency and critical speeds of hydro-turbine with its shaft, FEM model based on Ansys was used and observed that the gyroscopic effect has an effect on critical speed [2]. Vibration analysis of a simply supported turbine with shaft and bearing assembly was carried out to determine the natural frequency of the system. Sensitivity of various parameters such as length of shaft, diameter of the shaft and stiffness of the bearing were also performed to check the dynamic response of the assembly. Mathematical modelling for the equation of motion was carried out by calculating the Kinetic energy and potential energy of the shaft and a rotor disk [3]. Experimental approach to find the natural frequency and sensitivity of parameters as stated in above research was conducted. When the results were compared with the mathematical modelling, 4 percent error was noticed. Sensitivity of parameters shows a similar result as in above cited research [4]. Free vibration analysis of turbine assembly is performed by assuming the

model with single degree of freedom (SDOF) and continuous system. For SDOF type, Foppl/Jeffcott rotor modal and Rayleigh's Energy Method: Effective mass model Which are of discrete type models are used for calculation of natural frequency and for continuous system, continuous system model with total energy of system are used[5]. Vertical shaft turbine assembly was considered for the vibration analysis by performing the mathematical modelling. The effect of axial strain energy was also used during the calculation of total energy and derivation of equation of motion. Galerkin method was adopted to find the solution of the analytical method. To validate the mathematical model, model analysis is performed using Ansys [6]. Similar approaches were used for the vibration analysis for overhung assembly of turbine and shaft also [7].

From above literature, it is noticed that the researches had been performed to study the dynamic behavior of different arrangement of the turbine assembly such as simply supported, vertical axis and overhung system with single rigid mass body only with different mathematical approach such as FEM, effective mass model with assumed mode shape and Rayleigh energy methods. Actual hydro generator consist rotor body, turbine runner, fans and speed sensing devices as rigid mass body with stepped shaft. Again, each evidences of the literature prove that there will be different type of vibration pattern when the assembly of turbine, shaft, rotors and bearings differs.

In this research, a transverse vibration analysis of a hydro generator assembly which consist of stepped shaft, turbine runner, rotor and elastic bearing is performed to determine the lateral bending natural frequency at different mode of transverse vibration. A stationary shaft assembly is considered for the analysis which doesn't include the gyroscopic effect

due to absence of spinning motion. Thus, the stationary shaft is considered as a beam element. A different mathematical approach namely transfer matrix method is used for the analysis as this method contains simpler mathematical approach than the methodology presented in above cited literatures. The basic assumption of the method is that the rotor and runners are rigid thin disks.

2. Methodology

Conventional transfer matrix method famously known as Myklestad and Prohl Mehtod [8] with massless Euler-Bernoulli beam have been extensively used in the transverse vibration of the rotating shaft-disk system. In this study also, the same has been adopted as one of the analytical method. The disadvantages of this method are that the mass of the beam has to be assumed as a concentrated at different location. These concentrated points are taken as lumped rigid mass without rotary inertia and the shaft is treated as mass less Euler Bernoulli beam. Accuracy depends on how many concentrated points are defined for the beam segments.

To avoid the disadvantages of the conventional method, transfer matrix method based on Timoshenko beam theory is also formulated [9] in this research. Timoshenko beam is capable of handling the distributed mass of the shaft, rotary inertia and the shear deformation. The solution obtained from the transfer matrix method with Euler beam and Timoshenko beam is then compared with the results obtained from the commercial FEM software Simscale to validate the reliability of the mathematical model.

2.1 Transfer Matrix Formulation

In transfer matrix formulation, the assembly is discretized into number of beam segments, mass/disk and supports station. For them, the state variables such as transverse displacement, rotational displacement, bending moment and shear force at two end of the beam and two sides of the disk/mass are interrelated with the help of elementary transfer matrix of each components. Multiplication of all the elementary transfer matrix gives the overall transfer matrix of whole assembly which gives the natural frequency of the vibrating system after the application of the natural boundary condition of the system. The whole process is illustrated in the below sections.

2.2 Transfer matrix for Mass-Less Euler Bernoulli Beam

For the Euler Bernoulli beam, the mass of the beam is assumed to be concentrated at different location and the beam is considered as mass less with flexural rigidity.

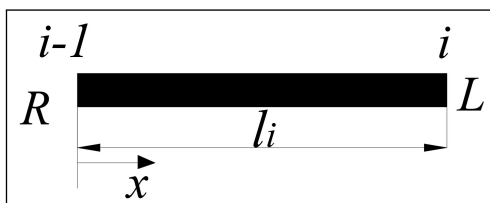


Figure 1: Beam Segment

Figure 1 shows the beam free body diagram of a beam for which the transfer matrix to relate the state variables are two ends are formulated with the help of elastic line theory and the equilibrium condition. The beam is considered as i^{th} element. Equation 1 gives the relation between the state variables at two ends of the shaft i.e. i^{th} and $(i-1)^{th}$ ends which can be further expressed as equation 2 [8].

$$\begin{Bmatrix} -v \\ \varphi_y \\ M \\ Q \end{Bmatrix}_i^L = \begin{bmatrix} 1 & l & \frac{l^2}{2EI} & \frac{l^3}{6EI} \\ 0 & 1 & \frac{l}{EI} & \frac{l^2}{2EI} \\ 0 & 0 & 1 & l \\ 0 & 0 & 0 & 1 \end{bmatrix} \begin{Bmatrix} -v \\ \varphi_y \\ M \\ Q \end{Bmatrix}_{i-1}^R \quad (1)$$

$$\{S\}_i^L = [F]_i \{S\}_{i-1}^R \quad (2)$$

with

$$\{S\}_i^L = \begin{Bmatrix} -v \\ \varphi_y \\ M \\ Q \end{Bmatrix}_i^L \quad \{S\}_{i-1}^R = \begin{Bmatrix} -v \\ \varphi_y \\ M \\ Q \end{Bmatrix}_{i-1}^R$$

$$[F]_i = \begin{bmatrix} 1 & l & \frac{l^2}{2EI} & \frac{l^3}{6EI} \\ 0 & 1 & \frac{l}{EI} & \frac{l^2}{2EI} \\ 0 & 0 & 1 & l \\ 0 & 0 & 0 & 1 \end{bmatrix}_i$$

In the above equation, v , φ_y , M and Q are the transverse displacement, angular displacement, bending moment and shear force considered for the single place motion. l is a length of the beam, E is a modulus of elasticity and I is a diametrical area moment of inertia. $[F]_i$ is a field matrix which relates the state variables $\{S\}$ at i^{th} and $(i-1)^{th}$ ends. R and L notations are also assumed for a beam ends as the i^{th} end of the beam is connected to the left side of the disk at that location and $(i-1)^{th}$ end of the beam is connected to the right side of the disk at that location.

2.3 Transfer matrix for Timoshenko Beam

Unlike Euler beam, Timoshenko beam considers the rotary inertia and the shear deformation of the beam. There is no need for concentrated mass assumption as in the case of Euler beam. Consider a beam segment which is vibrating in a single plane with frequency ω , having length l , cross-sectional area A , density ρ and second moment of inertia I . As shown in the figure 2, the slope of the centre line of the vibrating beam dv/dx is affected by both the bending moments and shear force. Bending moment rotates the face of cross-section with an angle φ_y and after then, the shear force act to turn the centre line to adopt the slope dv/dx . The angle between the centre line of beam and the line which is perpendicular to the face is a shear angle $\varphi_y + dv/dx$ which is caused by shear force. The mathematical expression for the shear force and bending moment is given by equation 3 and equation 4 respectively [10].

$$Q = \hat{k}GA(\dot{v} + \varphi_y) \quad (3)$$

$$M = EI \frac{d\varphi_y}{dx} \quad (4)$$

The notations G denotes the shear modulus of rigidity, \hat{k} denotes the shear deformation which depends upon the cross section of the beam, v denotes the transverse displacement, φ_y denotes the angular deformation, Q denotes shear force and M denotes the bending moments.

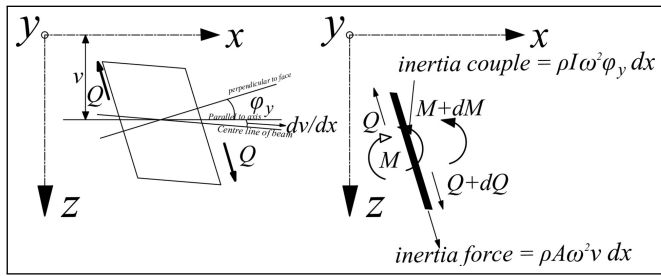


Figure 2: Effect of shear on beam deflection (left) and force acting on beam element (left)

The equilibrium equation for moment and shear force for an infinitesimally small beam segment having length dx can be expressed as equation 5 and equation 6 with reference to the figure 2 [9].

$$\frac{dM}{dx} = Q - \rho I \omega^2 \varphi_y \quad (5)$$

$$\frac{dV}{dx} = -\rho A \omega^2 v \quad (6)$$

substituting the derivative of equation 3 with respect to x and equation 4 in equation 6 and again, substituting the equation 4 and equation 6 to the derivative of equation 5, one obtains two differential equations for v and M . Eliminating M from these equation, one obtains fourth order differential equation in v which is expressed in equation 7.

$$\frac{d^4 v}{dx^4} + \frac{\rho A \omega^2}{EI} \left(\frac{EI}{\hat{k}GA} + \frac{I}{A} \right) \frac{d^2 v}{dx^2} - \frac{\rho A \omega^2}{EI} \left(1 - \frac{\rho I \omega^2}{\hat{k}GA} \right) v = 0 \quad (7)$$

Substitution of the following parameters on above fourth order equation leads to the characteristic equation with four roots $\pm \beta_1$ and $\pm j \beta_2$ which are shown in equation 8.

$$\sigma = \frac{\rho A \omega^2 l^2}{\hat{k}GA}, \alpha = \frac{\rho \omega^2 l^2}{E}, \tau^4 = \frac{\rho A \omega^2 l^4}{EI} \text{ and } v = C e^{\beta \frac{x}{l}} \quad (8)$$

$$\beta_1 = \sqrt{\left(-\frac{1}{2}(\sigma + \alpha) + \sqrt{\tau^4 + \frac{1}{4}(\sigma - \alpha)^2} \right)}$$

$$\beta_2 = \sqrt{\left(\frac{1}{2}(\sigma + \alpha) + \sqrt{\tau^4 + \frac{1}{4}(\sigma - \alpha)^2} \right)}$$

The solutions for the state variables is derived using the roots of the characteristics equation which is expressed in a matrix form in equation 9 [9].

$$\begin{Bmatrix} -v(x) \\ \varphi_y(x) \\ M(x) \\ Q(x) \end{Bmatrix} = \begin{bmatrix} T_{11} & T_{12} & T_{13} & T_{14} \\ T_{21} & T_{22} & T_{23} & T_{24} \\ T_{31} & T_{32} & T_{33} & T_{34} \\ T_{41} & T_{42} & T_{43} & T_{44} \end{bmatrix} \begin{Bmatrix} A \\ B \\ C \\ D \end{Bmatrix} \quad (9)$$

Where,

$$T_{11} = \frac{l^3 \beta_1}{\tau^4 EI} \sinh\left(\beta_1 \frac{x}{l}\right), T_{12} = \frac{l^3 \beta_1}{\tau^4 EI} \cosh\left(\beta_1 \frac{x}{l}\right)$$

$$T_{13} = -\frac{l^3 \beta_2}{\tau^4 EI} \sin\left(\beta_2 \frac{x}{l}\right), T_{14} = \frac{l^3 \beta_2}{\tau^4 EI} \cos\left(\beta_2 \frac{x}{l}\right)$$

$$T_{21} = \frac{l^2 (\sigma + \beta_1^2)}{\tau^4 EI} \cosh\left(\beta_1 \frac{x}{l}\right), T_{22} = \frac{l^2 (\sigma + \beta_1^2)}{\tau^4 EI} \sinh\left(\beta_1 \frac{x}{l}\right)$$

$$T_{23} = \frac{l^2 (\sigma - \beta_2^2)}{\tau^4 EI} \cos\left(\beta_2 \frac{x}{l}\right), T_{24} = \frac{l^2 (\sigma - \beta_2^2)}{\tau^4 EI} \sin\left(\beta_2 \frac{x}{l}\right)$$

$$T_{31} = \frac{l \beta_1 (\sigma + \beta_1^2)}{\tau^4} \sinh\left(\beta_1 \frac{x}{l}\right), T_{32} = \frac{l \beta_1 (\sigma + \beta_1^2)}{\tau^4} \cosh\left(\beta_1 \frac{x}{l}\right)$$

$$T_{33} = -\frac{l \beta_2 (\sigma - \beta_2^2)}{\tau^4} \sin\left(\beta_2 \frac{x}{l}\right), T_{34} = \frac{l \beta_2 (\sigma - \beta_2^2)}{\tau^4} \cos\left(\beta_2 \frac{x}{l}\right)$$

$$T_{41} = \cosh\left(\beta_1 \frac{x}{l}\right), T_{42} = \sinh\left(\beta_1 \frac{x}{l}\right)$$

$$T_{43} = \cos\left(\beta_2 \frac{x}{l}\right), T_{44} = \sin\left(\beta_2 \frac{x}{l}\right)$$

Further, the same can be expressed as equation 10.

$$S(x) = B(x) a \quad (10)$$

With reference to the above figure 1, using the same nomenclature for the ends of beam as above, a transfer matrix is formulated. At $(i-1)^{th}$ end, $x=0$ and at i^{th} end, $x=l$. Substituting these in equation 10 one by one and performing some manipulation, one obtains equation 11 to equation 13.

$$S_{i-1}^R = B(0) a \quad (11)$$

$$S_i^L = B(l) a \quad (12)$$

$$S_i^L = B(l) B^{-1}(0) S_{i-1}^R \quad (13)$$

The expanded form of equation 13 can be expressed as equation 14.

$$\begin{Bmatrix} -v \\ \varphi_y \\ M \\ Q \end{Bmatrix}_i^L = \begin{bmatrix} F_{11} & F_{12} & F_{13} & F_{14} \\ F_{21} & F_{22} & F_{23} & F_{24} \\ F_{31} & F_{32} & F_{33} & F_{34} \\ F_{41} & F_{42} & F_{43} & F_{44} \end{bmatrix} \begin{Bmatrix} -v \\ \varphi_y \\ M \\ Q \end{Bmatrix}_{i-1}^R \quad (14)$$

Where,

$$F_{11} = c_0 - \sigma c_2, F_{12} = l(c_1 - (\sigma + \alpha)c_3)$$

$$F_{13} = \frac{l^2 c_2}{EI}, F_{14} = \frac{l^3}{\tau^4 EI} [-\sigma c_1 + (\tau^4 + \sigma^2) c_3]$$

$$F_{21} = \frac{\tau^4 l}{c_3}, F_{22} = c_0 - \alpha c_2$$

$$F_{23} = \frac{l(c_1 - \alpha c_3)}{EI}, F_{24} = \frac{l^2 c_2}{EI}$$

$$F_{31} = \frac{\tau^4 EI c_2}{l^2}, F_{32} = \frac{EI}{l} [-\alpha c_1 + (\tau^4 + \alpha^2) c_3]$$

$$F_{33} = c_0 - \alpha c_2, F_{34} = l(c_1 - (\sigma + \alpha)c_3)$$

$$F_{41} = \frac{\tau^4 EI (c_1 - \sigma c_3)}{l^3}, F_{42} = \frac{\tau^4 EI c_2}{l^2}$$

$$F_{43} = \frac{\tau^4 l}{c_3}, F_{44} = c_0 - \sigma c_2$$

with,

$$c_0 = \Delta (\beta_2^2 \cosh \beta_1 + \beta_1^2 \cos \beta_2), c_1 = \Delta \left(\frac{\beta_2^2}{\beta_1} \sinh \beta_1 + \frac{\beta_1^2}{\beta_2} \sin \beta_2 \right)$$

$$c_2 = \Delta (\cosh \beta_1 - \cos \beta_2), c_3 = \Delta \left(\frac{\sinh \beta_1}{\beta_1} - \frac{\sin \beta_2}{\beta_2} \right)$$

$$\Delta = \frac{1}{\beta_1^2 + \beta_2^2}$$

Equation 14 can be further expressed as equation 15.

$$\{S\}_i^L = [F]_i \{S\}_{i-1}^R \quad (15)$$

$[F]_i$ is a field matrix which relates the state variables $\{S\}$ at i^{th} and $(i - 1)^{th}$ ends.

2.4 Transfer matrix for Disk and Elastic supports

For the analysis of the rotor and runner, a simplified disk element is considered to formulate the transfer matrix. Likewise, the bearings is modeled as elastic spring with specific stiffness values. The behavior of the vibrating disk or mass significantly impacts the natural frequency of the overall system. For i^{th} slender rigid disk with mass m and diametrical mass moment of inertia I_d or spring of the system vibrating with frequency denoted by ω , a transfer matrix is formulated to relate the state variables at two side for the station. For a free body diagram of the disk as shown in figure 3, the transfer matrix relation is expressed in equation 16 [11].

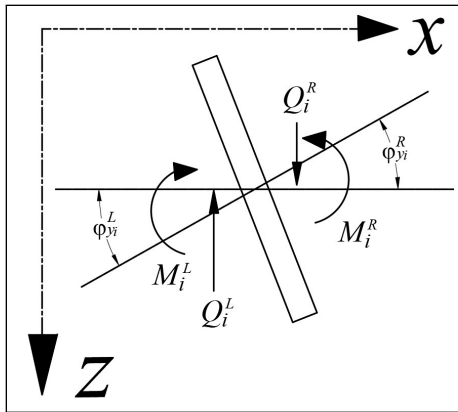


Figure 3: Free body diagram for disk element

$$\begin{Bmatrix} -v \\ \varphi_y \\ M \\ Q \end{Bmatrix}_i^L = \begin{bmatrix} 1 & 0 & 0 & 0 \\ 0 & 1 & 0 & 0 \\ 0 & -\omega^2 I_d & 1 & 0 \\ m\omega^2 & 0 & 0 & 1 \end{bmatrix}_i \begin{Bmatrix} -v \\ \varphi_y \\ M \\ Q \end{Bmatrix}_i^R \quad (16)$$

This above equation 16 can be express as equation 17, where $[P]_i$ is a point matrix which is a transfer matrix which relates the state variables at two sides of the disk. For a concentrated mass considered for the Euler-Bernoulli beam, the mass moment of inertia I_d is zero.

$$\{S\}_i^L = [P]_i \{S\}_i^R \quad (17)$$

For an elastic support with stiffness k as shown in figure 4, the the transfer matrix relation is expressed in equation 18 which is further expressed as equation 19 [11].

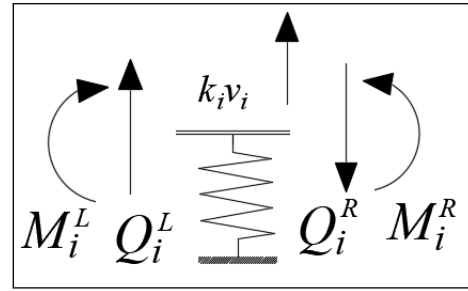


Figure 4: Free body diagram at spring support

$$\begin{Bmatrix} -v \\ \varphi_y \\ M \\ Q \end{Bmatrix}_i^L = \begin{bmatrix} 1 & 0 & 0 & 0 \\ 0 & 1 & 0 & 0 \\ 0 & 0 & 1 & 0 \\ -k & 0 & 0 & 1 \end{bmatrix}_i \begin{Bmatrix} -v \\ \varphi_y \\ M \\ Q \end{Bmatrix}_i^R \quad (18)$$

In equation , $[U]_i$ is a transfer matrix for elastic support relates the state variables at two sides of the same.

$$\{S\}_i^L = [U]_i \{S\}_i^R \quad (19)$$

2.5 Overall Transfer Matrix and Application of Boundary Condition

The overall transfer matrix for a hydrogenerator assembly is determined by multiplying all the elementary transfer matrix [11]. For the analysis, the hydro generator assembly shown in figure 5, with respective dimensions and parameters is considered. The discretization scheme with Euler-Bernoulli beam is shown in figure 6.

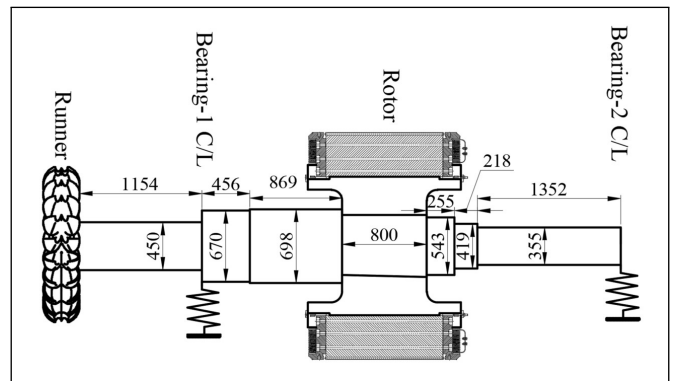


Figure 5: Hydro Generator Assembly Considered For Analysis

For this scheme, the masses of four beam segments, with lengths of 1.154 m, 0.870 m, 0.800 m, and 1.352 m, are considered to be located at the midpoint of each respective segment. In the case of the remaining segments, their masses are assumed to be concentrated at the end of the respective segments.

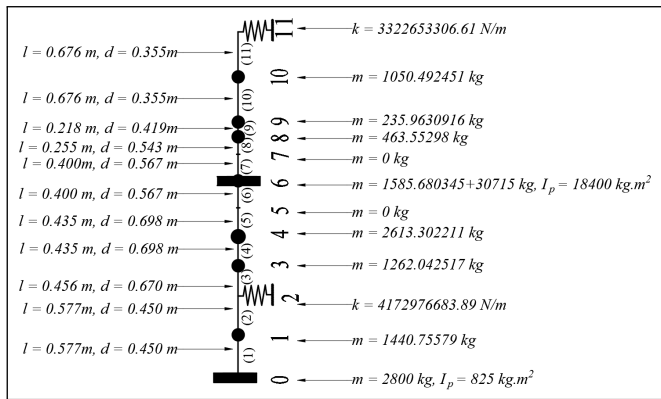


Figure 6: Discretization Scheme for Hydro generator assembly with Euler-Bernoulli Beam

The overall transfer matrix for this scheme can be expressed with equation 20. The naming for the stations and beams are as per the figure above.

$$\begin{aligned} \{S\}_{11}^R &= [U]_{11} [F]_{11} [P]_{10} [F]_{10} [P]_9 \\ & [F]_9 [P]_8 [F]_8 [P]_7 [F]_7 \\ & [P]_6 [F]_6 [P]_5 [F]_5 [P]_4 \\ & [F]_4 [P]_3 [F]_3 [U]_2 [F]_2 \\ & [P]_1 [F]_1 [P]_0 \{S\}_0^L \end{aligned} \quad (20)$$

Again, with the Timoshenko beam element, figure 7 shows the discretization scheme for which the overall transfer matrix is expressed as equation 21.

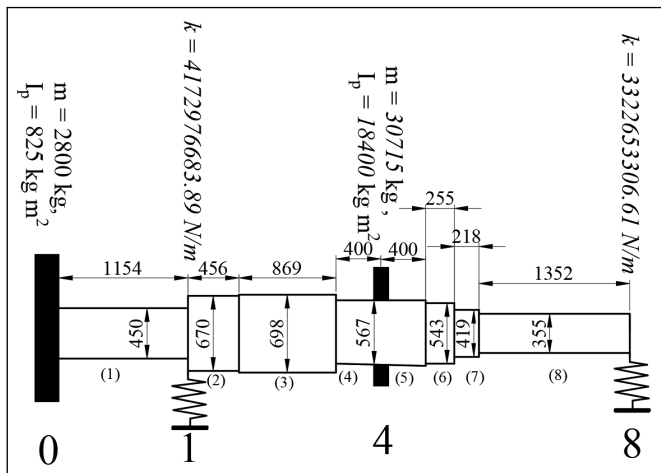


Figure 7: Discretization Scheme for Hydro generator assembly with Timoshenko Beam

$$\begin{aligned} \{S\}_8^R &= [U]_8 [F]_8 [F]_7 [F]_6 [F]_5 [P]_4 \\ & [F]_4 [F]_3 [F]_2 [U]_1 [F]_1 [P]_0 \{S\}_0^L \end{aligned} \quad (21)$$

In the context of hydro generator assembly lines, a prevalent boundary condition involves a free-free scenario, wherein the bending moment and shear force at both ends are maintained at zero. After the application of boundary conditions on equation 20 and equation 21 and expansion of the matrices, equation 22 is obtained. Single equation for expanded form is shown because the boundary condition and size of the matrix

is same for both the scheme. The subscripts 12 shall be used while solving for Euler beam scheme and 8 shall be used while solving for the Timoshenko beam scheme.

$$\begin{Bmatrix} -v \\ \varphi_y \\ 0 \\ 0 \end{Bmatrix}_{12 \text{ or } 8}^R = \begin{bmatrix} t_{11} & t_{12} & t_{13} & t_{14} \\ t_{21} & t_{22} & t_{23} & t_{24} \\ t_{31} & t_{32} & t_{33} & t_{34} \\ t_{41} & t_{42} & t_{43} & t_{44} \end{bmatrix} \begin{Bmatrix} -v \\ \varphi_y \\ 0 \\ 0 \end{Bmatrix}_0^L \quad (22)$$

On multiplication and some re-arrangements, one obtains equation 23 and equation 24.

$$\begin{Bmatrix} 0 \\ 0 \end{Bmatrix}_{12 \text{ or } 8}^R = \begin{bmatrix} t_{31} & t_{32} \\ t_{41} & t_{42} \end{bmatrix} \begin{Bmatrix} -v \\ \varphi_y \end{Bmatrix}_0^L \quad (23)$$

$$\begin{Bmatrix} -v \\ \varphi_y \end{Bmatrix}_{12 \text{ or } 8}^R = \begin{bmatrix} t_{11} & t_{12} \\ t_{21} & t_{22} \end{bmatrix} \begin{Bmatrix} -v \\ \varphi_y \end{Bmatrix}_0^L \quad (24)$$

Equation 23 represents an eigenvalue problem. Therefore, to obtain a non-trivial solution, it's necessary for equation 25 to equate to zero. Equation 25 is a function of natural frequency for transverse vibration ω . Hence, the natural frequencies associated with the bending vibration are the solutions of Equation 25. The first solution of Equation 25 that satisfy equation signifies the first mode natural frequency, second signifies the natural frequency for second mode and so on.

$$f(\omega) = \begin{vmatrix} t_{31} & t_{32} \\ t_{41} & t_{42} \end{vmatrix} = 0 \quad (25)$$

By choosing $\varphi_0^L = 1$ as the reference value for displacement, all the normalized state variables at station 0 are calculated and mode shape diagram is prepared.

3. Result and Discussion

For the discretized scheme shown in above figures, the natural frequency of transverse vibration for first three modes are calculated considering both euler and timoshenko beam. The dimensions shown in the figure 6 and figure 7 are in *millimeters*. Since, the material for the shaft/beam is mild steel, the modulus of elasticity E is taken as 210GPa and the Poisson's ratio μ is taken as 0.3. The shear deformation coefficient \hat{k} is calculated according to the mathematical relation available in reference [11]. Maple 2021 is used as a mathematical tool to evaluate the natural frequency. As the disks are considered thin, the diametrical mass moment of inertia I_d is taken as half of the polar mass moment of inertia I_p . The natural frequency calculated using euler beam and timoshenko beam model for the first three mode are shown in the table 1.

Table 1: Natural Frequency calculated for both Euler and Timoshenko Beam Scheme

Mode	Natural Frequency in Hz	
	Euler Beam Model	Timoshenko Beam Model
1	17.46	17.32
2	57.83	56.12
3	81.65	82.07

From above table, it can be noticed that the natural frequency calculated from the Timoshenko beam model are almost close to the Euler beam model for all three modes. This may be due to the lumped mass assumption considered for the uniformly distributed mass of the beam segment is almost close to the optimum discretization scheme, however, for other problems, the assumption technique applied in this paper might not be suitable and more point needs to be considered. Timoshenko beam model yields slightly lower value due to the consideration of the rotary inertia and shear deformation. For these above three modes of vibration, the normalized mode shape are plotted by calculating the normalized transverse displacement at each stations. The modes shape for first three modes for euler beam model is shown in figure 8 and the same for timoshenko beam model is shown in figure 9.

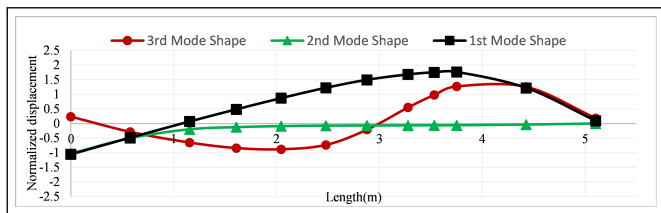


Figure 8: First three mode vibration mode shape considering Euler Beam

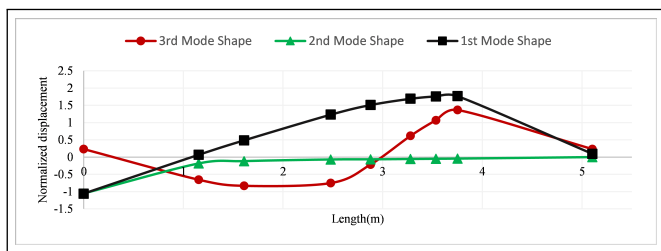


Figure 9: First three mode vibration mode shape considering Timoshenko Beam

From figure 8 and figure 9, it can be observed that the bending vibration mode are similar in nature for both the cases. The nodal points and antinodal points are at almost same location.

3.1 Frequency Analysis in SimScale and Comparison with Mathematical Approach

The dynamic analysis of the hydro generator assembly for free vibration is conducted using the finite element software SimScale. For an analysis, 3D model is prepared in Ansys Spaceclaim. To simulate the rotor winding and turbine runner, equivalent disks with identical mass and polar moment of inertia to the original components are modelled. The stiffness is provided as an Elastic Support boundary condition in the respective faces of the shaft. First three transverse vibration mode are considered in this paper. From the simulation, the natural frequency obtained for first three modes are shown in table 2.

Table 2: Natural Frequency obtained form SimScale for first three transverse vibration mode

Mode	Natural Frequency in Hz
1	20.01
2	49.9
3	90.54

The mode shape obtained for above three natural frequency are shown in figure 10, figure 11 and figure 12.

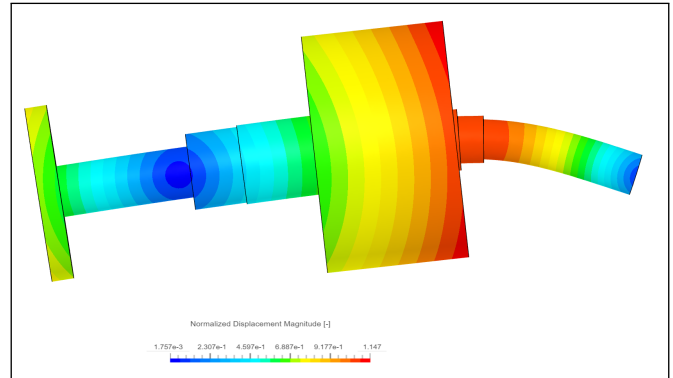


Figure 10: Vibration mode shape for frequency of 20.01 Hz

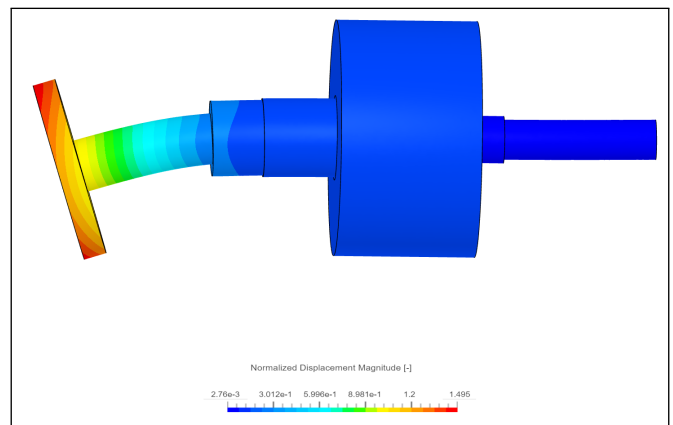


Figure 11: Vibration mode shape for frequency of 49.9 Hz

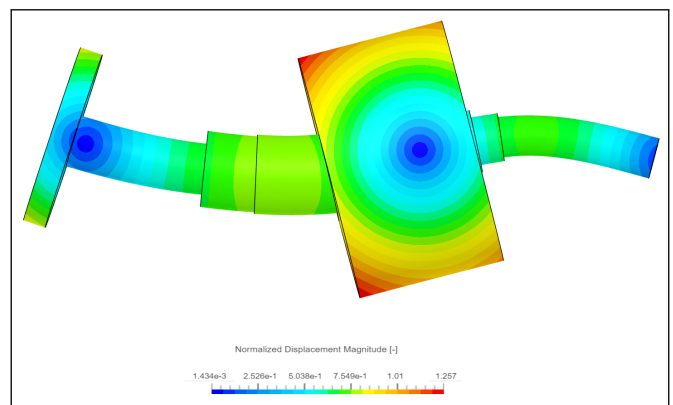


Figure 12: Vibration mode shape for frequency of 90.54 Hz

From the results obtained with mathematical approach and the results obtained from the SimScale, it can be noticed that

the results are almost close to each other for all three modes. However, it is also noticed that the results obtained from the Timoshenko Beam Scheme is more closest to the results from SimScale. This is due to the consideration of uniformly distributed mass of shaft and rotary inertia in the transfer matrix. Mode shapes natures are similar in Mathematical approach and SimScale. There is a minimal percentage variation in results from mathematical approach to the Finite element approach. This may be due to the assumption of disk as a thin disk and assumption of single plane vibration. However, there will be the effect due to thickness of the disk and the coupled plane vibration.

4. Conclusion and Future Recommendation

The natural frequency of a transverse vibration for a hydro-generator assembly is calculated using transfer matrix method involving the Euler-Bernoulli Beam and Timoshenko Beam. From the results obtained from the mathematical approach, it is noticed that the results obtained are close to the results obtained from FEM. The natural frequency calculated from the Euler beam models for the first three modes are 17.46 Hz, 57.83 Hz and 81.65 Hz and the same calculated with timoshenko beam models are 17.32 Hz, 56.12 Hz, 82.07 Hz. From the numerical model with Simscale, the natural frequency obtained are 20.01 Hz, 49.9 Hz and 90.54 Hz. Mode shapes obtained from the mathematical models and Simscale also exhibits similar nature. Thus, it can be concluded that the mathematical model presented in this paper can be efficiently employed for the natural frequency calculation of the hydro-generator assembly. Besides runner and rotor, the generator assembly also consists of the Fans, flywheel and excitors as a disk elements. Upon availability of the data regarding the mass and inertial, point matrices can be formulated for these items by a methodology described in this research and can be assembled in the overall transfer matrix for the calculation of the frequency. Again, this method is also capable of handling multiple number of bearing supports present in the assembly. Along with the free-free boundary condition, boundary condition for a simply supported and overhung assembly can also be incorporated in this method efficiently. As a future work, torsion mode can be added in transfer matrix and oil damping characteristic can also be added in the transfer matrix of the supports. Again, the

thickness parameter of disk can also be added in the point matrix.

Acknowledgments

The authors are thankful to Department of Automobile and Mechanical Engineering, Thapathali Campus for providing continuous support during this study.

References

- [1] John M Vance. *Rotordynamics of turbomachinery*. John Wiley & Sons, 1991.
- [2] Bing Bai, Lixiang Zhang, Tao Guo, and Chaoqun Liu. Analysis of dynamic characteristics of the main shaft system in a hydro-turbine based on ansys. *Procedia Engineering*, 31:654–658, 2012. International Conference on Advances in Computational Modeling and Simulation.
- [3] Aman Rajak, Prateek Shrestha, Manoj Rijal, Bishal Pudasaini, and Mahesh Chandra Luitel. Dynamic analysis of pelton turbine and assembly. In *Proceedings of IOE Graduate Conference*, 2014.
- [4] Akshay D. Shinde and S.N. Shelke. A review on dynamic analysis of pelton wheel turbine. 2016.
- [5] Laxman Motra and Mahesh Chandra Luitel. Free vibration analysis of selected pelton turbine using dynamic approach. In *Proceedings of IOE Graduate Conference*, 2017.
- [6] Rujan Timsina and Mahesh Chandra Luitel. Dynamic response of vertical shaft pelton turbine unit for free vibration. In *Proceedings of IOE Graduate Conference*, 2020.
- [7] Kamal Pokharel and Mahesh Chandra Luitel. Dynamic response of overhung pelton turbine unit for free vibration. In *Proceedings of IOE Graduate Conference*, 2019.
- [8] JS Rao. *Rotor dynamics*. New Age International, 1996.
- [9] Eduard Pestel, Frederick A. Leckie, and E. F. Kurtz. Matrix methods in elastomechanics. 1963.
- [10] Xiaoting Rui, Guoping Wang, Yuqi Lu, and Laifeng Yun. Transfer matrix method for linear multibody system. *Multibody System Dynamics*, 19:179–207, 2008.
- [11] R. Tiwari. *Rotor Systems: Analysis and Identification*. CRC Press, Taylor & Francis Group, 2017.